ATLANTIS PRESS

Advances in Computer Science Research, volume 87

3rd International Conference on Mechatronics Engineering and Information Technology (ICMEIT 2019)

Detection of Facial Wrinkle based on Improved Maximum Curvature Points in Image Profiles

Die Zhou [a], Shuo Zhao [b]

School of Software Engineering, Chongqing University of Posts and Telecommunications, Chongqing 400000, China.

[a]894948360@qq.com, [b]991008055@qq.com

Abstract. Face wrinkles, as an important sign of aging and the focus of anti-aging, have great research significance in detecting them. However, rough skin result in more noises, and the intensity difference between the fine wrinkles and the skin background is too small, which ultimately leads to low detection rate of wrinkles. An improved maximum curvature method is proposed for wrinkle detection. Firstly, the intensity gradient caused by wrinkles is highlighted by combining the image features of Gabor filter bank and Frangi filter. Then, the filtered result image is binarized, and the connected component eccentricity distribution is counted to judge the wrinkle feature extraction effect. According to the effect of wrinkle feature extraction, the image is selected, and the local maximum curvature of the cross-sectional contour is calculated to detect wrinkles. At the same time, combined with the complex geometric features of wrinkles, the connection method in the algorithm is improved. Compared with the existing wrinkle detection methods, the proposed method greatly improves the detection rate of wrinkles, especially in rough skin images.

Keywords: wrinkle detection; Gabor filter bank; Frangi filter; maximum curvature.

1. Introduction

Wrinkle is one of the signs of skin aging, and its detection plays an important role in the aging applications. For example, age estimation, age simulation and recognition across aging[1]. Wrinkles are three-dimensional features of skin surface, which are extremely symbolic features. Therefore, it also has applications in face recognition, expression recognition, analysis, expression synthesis[2].

Most wrinkle detection methods regard wrinkles as skin texture, and only a few methods regard wrinkles as curve objects. But wrinkles are not the same as skin texture. Skin texture is innate, uniform and repetitive. Wrinkles are caused by skin aging and long-term contraction of facial muscles. Therefore, wrinkles are a curve object with certain intensity and geometric constraints.

There are two main methods to detect wrinkles as curve objects: stochastic and deterministic modeling techniques. Batool[3] proposed a generative stochastic model for wrinkles using Marked Point Processes. This method requires a lot of computing time and depends on the placement of the initial line segment. Batool[4] proposed a deterministic approach based on image morphology for fast localization of facial wrinkles. The accuracy and calculation of the method have been improved. However, under the rough skin image or high-resolution image, the wrinkle feature extraction is poor and the noise is more, resulting in a low detection rate of wrinkles. Ng[5] proposed an algorithm for detecting wrinkles using a hybrid Hessian filter. This method is only suitable for detecting rough wrinkles in horizontal direction, so it has great limitations. Ng[6] proposed a line tracking method for wrinkle detection based on their original hybrid Hessian filter. The detection rate has been improved compared with the original algorithm, but the problem of low detection rate of fine wrinkles has not been completely solved.

2. Improved Maximum Curvature Points in Image Profiles

The steps of wrinkle detection in this paper include feature extraction, wrinkle feature extraction effect determination, wrinkle centerline location and subsequent denoising processing.

2.1 Gabor Filter Bank Combined with Frangi Filter

The real Gabor filter kernel oriented in a 2D image plane at angle α is given by[4]:

$$g(x_1,x_2)=\frac{1}{2\pi\sigma_{x_1}\sigma_{x_2}}\exp[\frac{-1}{2}(\frac{x_1^{'2}}{\sigma_{x_1}^2}+\frac{\gamma x_2^{'2}}{\sigma_{x_2}^2})]\cos(2\pi f x_1^{'}) \tag{1}$$

Let $\{g_k(x_1,x_2),k=0,...,K-1\}$ denote the set of real Gabor filters oriented at angles $\alpha_K=-\pi/2+k\pi/K$ where K is the total number of equally spaced filters over the angular range. Then Gabor features can be obtained by convolving this Gabor filter bank with the given image. Let $I(x_1,x_2)$ denote the input grayscale image, and $I_k^F(x_1,x_2)$ denote the image filtered by the filter $g_k(x_1,x_2)$ .The corresponding maximum amplitude among the filtered responses is given as[4]:

$$I^{'}(x_1,x_2)=\max_k I_k^F(x_1,x_2) \tag{2}$$

Then normalize it and let a denote it to the range [0,1], let $I_g^N(x_1,x_2)$ denote it.

Frangi filter [7] is based on Hessian matrix. First, the Hessian matrix is calculated. let $I(x_1,x_2)$ denote the input grayscale image, its Hessian matrix is H . Then, two eigenvalues λ_1, λ_2 of the Hessian matrix are calculated. And based on the two eigenvalues sought, construct two variables R_b , S . Construct a filter response function based on R_b , S :

$$v_o(s)=\begin{cases}0, & \lambda_2>0\\ \exp(-\frac{R_b^{\,2}}{2\beta^2})(1-\exp(-\frac{s^2}{2c^2})) & \end{cases} \tag{3}$$

In order to combine this with the Gabor filter bank, it is normalized, and let $I_f^N(x_1,x_2)$ denote.

The filtered normalized results are combined as follows.

$$GF(x_1,x_2)=I_g^N(x_1,x_2)+p*I_f^N(x_1,x_2) \tag{4}$$

Because in the actual wrinkle image, most of it is still finer wrinkles. The parameter p is set to a value in the range (0, 1) to suppress the response of the Frangi filter while highlighting the Gabor filter bank response to some extent.

2.2 Judgment of Wrinkle Feature Extraction Effect

The geometric shape of the wrinkles appears as a curved object, so the eccentricity should be higher. The filtering result is binarized. If the wrinkle feature extraction effect is good, the eccentricity of most of the connected components is higher. On the contrary, if the effect of wrinkle feature extraction is poor, the eccentricity of only a few connected components is higher.

N_8 and N_9 denote the percentage of the number of connected components with an eccentricity of 0.8 to 0.9 and 0.9 to 1, respectively. When $N_9>0.25$ and $N_9/N_8>0.7$, the wrinkle feature is extracted well, then the filtered image is used as the image profiles to calculate the maximum curvature points. Otherwise, the gray image is used as the image profiles.

2.3 Maximum Curvature Points in Image Profiles

The maximum curvature method consists of three steps: firstly, extracting the center positions of wrinkles; secondly, connecting the center position of wrinkles; finally, Labeling of the image[8].

In the step of extracting the wrinkle center positions, the curvature of the cross-sectional profile is calculated first. $I(x_1,x_2)$ is the input wrinkle image, $p_f(z)$ be the cross-sectional profile acquired

from $I(x_1, x_2)$ at any direction and position, where z is a position in a profile. The curvature $k(z)$, can be represented as[8]

$$k(z) = \frac{d^2 p_f(z)/dz^2}{\{1+(dp_f(z)/dz)^2\}^{\frac{3}{2}}} \tag{5}$$

Then, the local maximum points of $k(z)$ in each concave area are calculated, which are defined as z_i', where $i = 0,1,...,N-1$, and N is the number of local maximum points.

The score of the local maximum point, which indicates the probability of the point on the wrinkle centerline, and is calculated as follows[8]:

$$S_{cr}(z_i') = k(z_i') \times W_r(i) \tag{6}$$

where $W_r(i)$ is the width of the region where the curvature is positive and one of the z' is located. Scores are assigned to a plane, V, which is a result of the emphasis of the wrinkles[8].

$$V(x_i', y_i') = V(x_i', y_i') + S_{cr}(z_i') \tag{7}$$

According to the above steps, all the profiles in four directions (horizontal, vertical and the two diagonals) are also analyzed. Finally, four detection results of wrinkle center position are obtained: V_{d1}, V_{d2}, V_{d3} and V_{d4}, where d_1, d_2, d_3 and d_4 represent horizontal, vertical, and two diagonal directions, respectively.

To connect the center position, Miura use the operation as shown as fallows[8].

$$C_{d1}(x,y) = \min\{\max(V(x+1,y), V(x+2,y)) + \max(V(x-1,y), V(x-2,y))\} \tag{8}$$

The calculation is repeated for four directions yielding C_{d1}, C_{d2}, C_{d3} and C_{d4}.The connection of the original method is horizontal. The wrinkles in different part have different trends. And there are one or two major wrinkle directions in a wrinkle image. Therefore, the direction of the connection needs to be based on the specific direction of wrinkles in the wrinkle image. And the connection operations in the other three directions are as follows:

$$C_{di}(x,y) = \min\left\{\max\left(V_{di}(x,y+1), V_{di}(x,y+2)\right) + \max\left(V_{di}(x,y-1), V_{di}(x,y-2)\right)\right\} \tag{9}$$

$$C_{di}(x,y) = \min\left\{\max\left(V_{di}(x+1,y-1), V_{di}(x+2,y-2)\right) + \max\left(V_{di}(x-1,y+1), V_{di}(x-2,y+2)\right)\right\} \tag{10}$$

$$C_{di}(x,y) = \min\left\{\max\left(V_{di}(x+1,y-1), V_{di}(x+2,y-2)\right) + \max\left(V_{di}(x-1,y+1), V_{di}(x-2,y+2)\right)\right\} \tag{11}$$

This paper calculates the average score of the cross-sectional profile in each direction, reflects the main trend of wrinkles, and finally determines the connection direction. The calculation of the average score is as follows.

$$AS_{d1} = \frac{\sum_{i=0}^{N-1} S_{cr}(z_i')}{N} \tag{12}$$

Where N is the number of local maximum points. $S_{cr}(z_i')$ is the score of the center positions.

The average fractions of cross-sectional profile in four directions are calculated respectively: AS_{d1}, AS_{d2}, AS_{d3} and AS_{d4} he average scores of the above four directions are arranged in descending order, the ratio of the maximum and the second largest values $K_A = S1/S2$.

When $K_A < 1.3$,the connection directions $DM1$ and $DM2$ are perpendicular to the direction of $S1$ and $S2$. The connection result in two directions is $CDM1_{di}$, $CDM2_{di}$, where i represents the wrinkle center positions detection result based on the cross-sectional profile in four directions. Finally, the connection result $G(x,y) = \max_{i=1}^{4}(CDM1_{di}, CDM2_{di})$.

When $K_A \geq 1.3$, the connection directions DA is perpendicular to the direction of $S1$. The connection result is $G(x,y) = \max_{i=1}^{4}(CDA_{di})$.

The result $G(x,y)$ is binarized by using a threshold. Pixels smaller than the threshold are labeled as background, and pixels larger than or equal to the threshold are labeled as wrinkles.

The binary image is post-processed based on some geometric constraints of the wrinkle curve objects. First, remove some isolated or too small connected components. Then, the connected component having an eccentricity of less than 0.95 is removed.

3. Experimental Results and Analysis

The experimental data in this paper consists of two parts. First, high-resolution face images captured using the magic mirror skin detector. The wrinkle regions of the collected face images are cropped, including forehead, eyebrow, eye and mouth. Some wrinkle region images have been downloaded on the network, and the resolution of such images is low.

Four images were randomly selected from the wrinkle region images of forehead, eyebrow, eye and mouth, and compared with Batool [4], Ng [6] and Miura [8]. Fig.1, Fig. 2, Fig. 3 and Fig. 4 show the experimental results of wrinkle detection in four facial wrinkle regions using the above methods. Since the wrinkle detection method proposed by N g is only suitable for detecting wrinkles in the forehead region, it is only compared with the detection result in the forehead region.

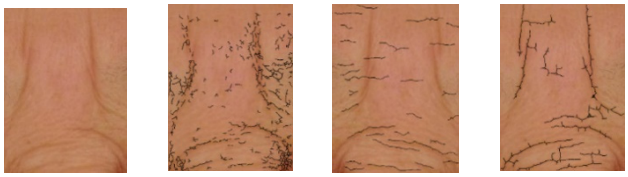

(a)Original (b) Batool (c) Miura (d) proposed

Fig. 1 comparison of detection results in brow

(a)Original (b) Batool (c) Miura (d) proposed

Fig. 2 comparison of detection results in mouth

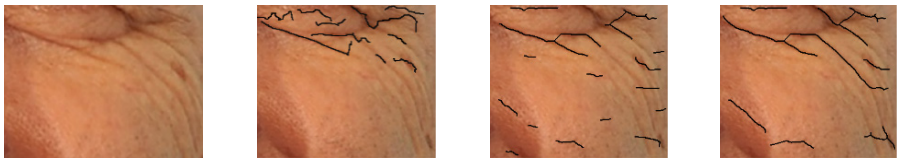

(a)Original Image (b) Batool (c) Miura (d) proposed

Fig. 3 comparison of detection results in eye

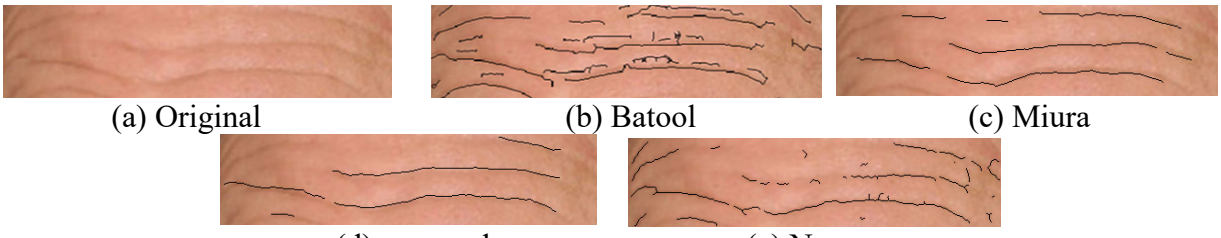

(a) Original (b) Batool (c) Miura

(d)proposed (e) Ng

Fig. 4 comparison of detection results in forehead

In order to analyze and compare the overall detection ratio and false alarm ratio of the above-mentioned wrinkle detection method, the average value of the detection ratio and false alarm ratio of each wrinkle method in each region is calculated, as shown in Table 1 and Table 2.

Table 1. Comparison of detection ratio

	forehead	brow	eye	mouth	Average detection ratio
Choon-Ching Ng	0.5303	--	--	--	--
Nazre Batool	0.5225	0.4678	0.5893	0.4176	0.4993
Naoto Miura	0.4113	0.2303	0.3621	0.1461	0.2875
proposed	**0.6429**	**0.6737**	**0.6439**	**0.5861**	**0.6367**

Table 2. Comparison of false alarm ratio

	forehead	brow	eye	mouth	Average false alarm ratio
Choon-Ching Ng	0.1049	--	--	--	--
Nazre Batool	0.0661	0.0628	0.0568	0.0549	0.0602
Naoto Miura	0.0124	0.0129	0.0107	0.0105	0.0116
proposed	**0.0143**	**0.01978**	**0.0144**	**0.0176**	**0.01652**

As can be seen from Table 1, in the four wrinkle regions, the detection ratio of this paper is significantly higher than that of Choon-Ching Ng, Nazre Batool and Naoto Miura. Especially compared with Naoto Miura algorithm, it has a relatively high detection rate for the forehead region, because the main trend of wrinkles in this region is horizontal, while the detection rate for the other three regions is very low. So, the improvement of the connection method on this article is effective.

As can be seen from Table 4.3, Choon-Ching Ng's algorithm false alarm ratio is higher than other methods. The false alarm ratio of this paper is lower than that of Choon-Ching Ng and Nazre Batool. The detection rate is 0.00492 more than the Naoto Miura method, but the false alarm ratio of this paper is also within the acceptable range compared to the detection ratio of 0.03494.

4. Summary

In this study, a method combining Gabor filter bank and Frangi filter is proposed to extract image features, and the maximum curvature method is improved for wrinkle detection. After the image features are binarized, the connected component eccentricity distribution is calculated. According to the distribution results, the corresponding images are selected, and the local maximum curvature points of the cross-sectional profile is used to detect the wrinkles. In order to adapt to the complex geometry of wrinkles, the connecting step in the algorithm are improved. Compared with the existing wrinkle detection methods, the proposed method greatly improves the detection rate of wrinkles, especially in rough skin images.

References

[1]. Jeong S G, Tarabalka Y, Zerubia J. Marked point process model for facial wrinkle detection[C]// IEEE International Conference on Image Processing. Paris, 2015, p. 1391-1394.

[2]. Xie W, Shen L, Jiang J. A novel transient wrinkle detection algorithm and its application for expression synthesis[J]. IEEE Transactions on Multimedia. Vol. 19 (2017) No. 2, p. 279-292.

[3]. Batool N, Chellappa R. Modeling and detection of wrinkles in aging human faces using marked point processes[C]// European Conference on Computer Vision. Florence, 2012, p. 178-188.

[4]. Batool N, Chellappa R. Fast detection of facial wrinkles based on Gabor features using image morphology and geometric constraints[J]. Pattern Recognition. Vol. 48 (2015) No. 3, p. 642-658.

[5]. Ng C C, Yap M H, Costen N, et al. Automatic Wrinkle Detection Using Hybrid Hessian Filter[C]// Asian Conference on Computer Vision. Florence, 2014, p. 609-622.

[6]. Ng C C, Yap M H, Costen N, et al. Wrinkle detection using hessian line tracking[J]. IEEE Access. Vol. 3 (2015) No. 2, p. 1079-1088.

[7]. Frangi R F, Niessen W J, Vincken K L, et al. Multiscale vessel enhancement filtering[C]// International Conference on Medical Image Computing and Computer-Assisted Intervention. Florence, 2000, p. 130-137.

[8]. Miura N, Nagasaka A, Miyatake T. Extraction of finger-vein patterns using maximum curvature points in image profiles[J]. Ieice Transactions on Information and Systems. Vol. 90 (2007) No. 8, p. 1185-1194.